DOI: 10.1002/ejic.200600819

Structural Distortion and Magnetic Behavior in Cyanide-Bridged $Fe^{III}_2Ni^{II}_2$ Complexes

Dongfeng Li,[a] Rodolphe Clérac,[b] Guangbin Wang,[c] Gordon T. Yee,[c] and Stephen M. Holmes*[a]

Keywords: Cyanometalate / Magnetism / Single-molecule magnets / Pyrazolylborate / Magnetic relaxation

The X-ray structure, spectroscopic, and magnetic properties of a cyanide-bridged complex, $\{[(Tp^*)Fe^{III}(CN)_3]_2[Ni^{II}(bipy)_2]_2[OTf]_2\}\cdot 2H_2O$ (**2**) are described [Tp^* = hydridotris(3,5-dimethylpyrazol-1-yl)borate; bipy = 2,2′-bipyridine; OTf = trifluromethanesulfonate]. Magnetic measurements indicate that **2** exhibits an $S = 3$ ground state and slow relaxation of the magnetization. Magnetostructural comparisons to the more symmetrical analog $\{[(Tp^*)Fe^{III}(CN)_3]_2[Ni^{II}(DMF)_4]_2[OTf]_2\}\cdot 2DMF$ (**1**) are also described. Surprisingly, the magnetic properties of **1** and **2** are similar despite the presence of a non-planar $\{Fe^{III}_2Ni^{II}_2(\mu\text{-}CN)_4\}$ core and severely distorted Ni^{II} coordination sphere in **2**, suggesting that the Ni^{II} centers play a minor role in the slow magnetization relaxation behavior of the clusters.

Introduction

Single-molecule magnets (SMMs) have remained an active area of research over the last decade due to their unusual magnetic properties and potential use in molecule-based information storage devices.[1–5] The largest family of SMMs contain anisotropic metal centers linked by oxo- and carboxylate ligands, with $Mn_{12}O_{12}(O_2CMe)_{16}(OH_2)_4$ being the best characterized example. The complex exhibits superparamagnetic-like behavior owing to the large spin ground state and Ising-type anisotropy derived from the anisotropic metal centers present.[1–5]

Several polynuclear cyanide-bridged complexes that exhibit slow relaxation of the magnetization containing $[fac\text{-}LM(CN)_3]^{n-}$ units have been described over the last few years, where L = 1,4,7-trimethyltriazacyclononane, 1,1,1-tris(diphenylphosphanomethyl)ethane, tris(3,5-dimethylpyrazolyl)borate, and tris(pyrazolyl)borate.[5–15] Among these, we previously reported that $\{[(Tp^*)Fe^{III}(CN)_3Ni^{II}(DMF)_4]_2[OTf]_2\}\cdot 2DMF$ (**1**) exhibits slow relaxation of the magnetization with an apparent blocking temperature near 1.8 K [Tp* = hydridotris(3,5-dimethylpyrazol-1-yl)borate, OTf = trifluoromethanesulfonate, DMF = dimethylformamide].[7]

Recently, Rogez et al. reported that distorted six-coordinate nickel(II) complexes can exhibit very large and negative D values ($D = -10.1\ cm^{-1}$),[16] while Accorsi et al. demonstrated that anisotropy barriers in tetrairon(III) single-molecule magnets can be systematically tuned by ligand substitution; Brechin et al. has demonstrated that $[Mn^{III}]_6$ clusters can also be tuned by this strategy.[17] We rationalized that replacement of DMF ligands present in **1** for rigid, sterically demanding ancillary ligands such as 2,2′-bipryidine (bipy), would significantly distort the Ni^{II} coordination sphere and afford greater single-ion anisotropy. If greater single-ion anisotropy of the Ni^{II} centers translates into greater molecular anisotropy, then the energy barrier and the blocking temperature of the $\{Fe^{III}_2Ni^{II}_2\}$ complexes may also be systematically tuned. In the present Communication, we compare the structures and spectroscopic and magnetic properties of two rectangular complexes, $\{[(Tp^*)Fe^{III}(CN)_3]_2[Ni^{II}(L_n)]_2[OTf]_2\}$ (L_n = 4 DMF, **1**; 2 bipy, **2**), that exhibit $S = 3$ ground states and slow relaxation of the magnetization.[7,18]

Results and Discussion

Synthesis and Characterization

Treatment of $\{[(Tp^*)Fe^{III}(CN)_3]_2[Ni^{II}(DMF)_4]_2[OTf]_2\}\cdot 2DMF$ (**1**)[7] with 2,2′-bipyridine (bipy) in MeCN/MeOH (v/v, 1:1) mixtures cleanly affords $\{[(Tp^*)Fe^{III}(CN)_3]_2[Ni^{II}(bipy)_2]_2[OTf]_2\}\cdot 2H_2O$ (**2**) as a red crystalline solid.[18] The infrared spectrum of **2** exhibits intense ν_{BH} and ν_{CN} stretching absorptions at 2553, 2158 and 2128 cm^{-1}, respectively, that are shifted to higher energies relative to those seen for $[NEt_4][(Tp^*)Fe^{III}(CN)_3]$ (2549 and

[a] University of Kentucky, Department of Chemistry, Lexington, Kentucky 40506-0055, USA
Fax: +1-859-323-1069
E-mail: smholm2@uky.edu
[b] Centre de Recherche Paul Pascal, UPR-CNRS 8641, 33600 Pessac, France
[c] Virginia Polytechnic and State University, Department of Chemistry, Blacksburg, Virginia 24061, USA
Supporting information for this article is available on the WWW under http://www.eurjic.org or from the author.

2115 cm^{-1}); the ν_{CN} stretches are tentatively assigned as bridging and terminal cyanides, respectively.[6–9,19–22] In comparison the energies of the ν_{BH} (2547 cm^{-1}) and ν_{CN} (2170, 2163, and 2120 cm^{-1}) stretching absorptions[7] for **1** are found at higher energies than those in **2**, suggesting that either depopulation of the 5σ cyanide orbital is less efficient, and/or more efficient π back-bonding occurs in **2**.[29]

Compound **2** crystallizes in the triclinic $P\bar{1}$ space group and is structurally related to **1**.[23] The cationic rectangular complex consists of two octahedral [*cis*-$Ni^{II}(bipy)_2]^{2+}$ centers that are linked to two adjacent $[(Tp^*)Fe^{III}(CN)_3]^-$ anions (Figure 1) through bridging cyanides. The Fe–C≡N bond angles and Fe–C and Ni–N bond lengths are comparable in **1** and **2**, respectively (Table 1). The structural details of **1** have been previously reported.[7]

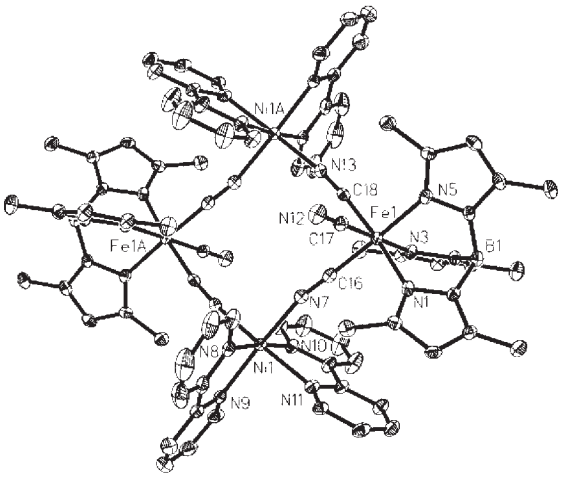

Figure 1. X-ray structure of **2**. Thermal ellipsoids are at the 50% level and all anions, lattice solvent, and hydrogen atoms are omitted for clarity.

Table 1. Selected bond lengths [Å] and angles (°) for **1** and **2**.

Compound **1**			
Fe1–C16	1.928(5)	C16–Fe1–C18	85.4(2)
Fe1–C18	1.927(5)	N9–Ni1–N7A	92.3(1)
Ni1–N9	2.039(4)	Ni1–N9–C18	176.9(4)
		Fe1–C16–N7	177.3(4)
Compound **2**			
Fe1–C16	1.920(5)	C16–Fe1–C18	83.8(2)
Fe1–C17	1.932(5)	N7–Ni1–N13A	95.1(2)
Ni1–N7	2.063(4)	Ni1–N7–C16	167.1(4)
		Fe1–C16–N7	178.0(4)

In **2**, the Ni1–N bond lengths for the *cis* cyanides are 2.042(4) (Ni1–N7) and 2.063(4) Å (Ni1–N13A), while those for the bipyridine, range from 2.074(4) (Ni1–N8) to 2.112(4) Å (Ni1–N11), respectively (Table 1). The bridging cyanide Fe1–C bond lengths, 1.916(5) and 1.920(5) Å, are nearly equivalent, while the longest distance [1.932(5) Å] is found for the terminal cyanide (Fe1–C17).[18] The bridging Fe–C≡N bond angles range from 173.4(4)° (Fe1–C18–N13) to 178.0(4)° (Fe1–C16–N7), while the terminal cyanide (Fe–C17–N12) is nearly linear [178.1(4)°]. The Ni–N≡C bond angles are significantly bent, ranging from 167.1(4)° (Ni1–N7–C16) to 171.9(3)° (Ni1–N13A–C18A), respectively; the N–Ni–N bond angles of the [*cis*-$Ni^{II}(bipy)_2(\mu\text{-}NC)_2$] fragments range from 78.5(2) to 98.8(2)°. We presume that significant steric congestion, between the Tp* and bipy ligands, afford dissimilar N7–Ni1–N13A [95.1(2) Å] and C16–Fe1–C18 [83.8(2) Å] bond angles, and a distorted nonplanar $\{Fe^{III}_2Ni^{II}_2(CN)_4\}$ framework. The intramolecular Fe1···Fe1A, Fe1···Ni1, and Ni1···Ni1A contacts are 7.628(1), 5.097(1), and 6.733(1) Å, respectively, while the closest intermolecular contacts between terminal cyanides and bipy rings are 3.297(1) Å (Figure 1).[18] In comparison the closest intercluster contacts for **1** are 4.363(3) Å.[7]

The structural distortions of **1** and **2** can be further described by the torsion angles present in each complex.[18] Looking down the Ni1(μ-CN)Fe1 axis and considering only the inner-sphere atoms coordinated to each metal center in **1** for clarity, the N7A–Ni1–Fe1–N7, O1A–Ni1–Fe1–N3, O1B–Ni1–Fe1–N5, and O1D–Ni1–Fe1–N8 torsion angles are ca. 3.6, 7.7, 11.3, and 8.4°, respectively, suggesting that **1** adopts a rather flat rectangular structure (Figure 2). In comparison, **2** exhibits a very distorted $\{Fe^{III}_2Ni^{II}_2(\mu\text{-}CN)_4\}$ core, as indicated by the nonlinear μ-CN bridges and large angular deviations from an eclipsed configuration of coordinated heteroatoms present on the Fe and Ni centers; the N11–Ni1–Fe1–N1, N8–Ni1–Fe1–N12, N13–Ni1–Fe1–N13A, and N10–Ni1–Fe1–N3 angles are 24.5, 18.4, 5.5, and 10.6°, respectively (Figure 1).[18]

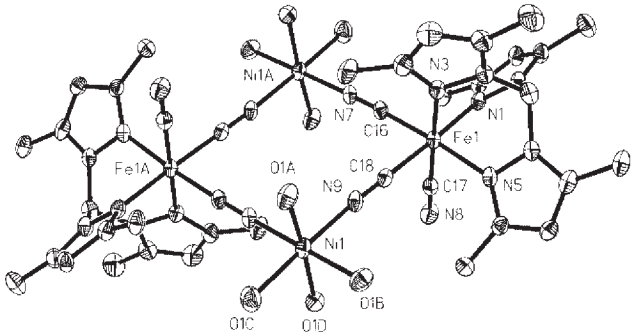

Figure 2. X-ray structure of **1**. Thermal ellipsoids are at the 50% level and all anions, lattice solvent, and hydrogen atoms are omitted for clarity.

Magnetic Characterization

The χT vs. T data suggests that the Fe^{III} (S = 1/2) and Ni^{II} (S = 1) centers in **2** are ferromagnetically coupled (Figure 3), because the χT product gradually increases from 3.8 $cm^3\,K\,mol^{-1}$ (300 K), reaching a maximum value of 7.7 $cm^3\,K\,mol^{-1}$ at 7 K. Below 7 K, χT decreases towards a minimum value of 6.6 $cm^3\,K\,mol^{-1}$ at 1.83 K.[6–9,21,22] Based on the tetranuclear structure of **2**, the magnetic data has been modeled using an isotropic Heisenberg model in the weak field approximation.[24–26] The theoretical susceptibility has been deduced from application of the van Vleck equation to the Kambe method, by the following spin Ham-

iltonian: $H = -2J\{(S_1 + S_2)\cdot(S_3 + S_4)\}$,[27,28] where J is the isotropic exchange interaction between Fe^{III} and Ni^{II} sites and S_i is the spin operator for each metal center (S_i = 1, Ni^{II}, with i = 1–2; S_i = 1/2, Fe^{III}, with i = 3–4). The best set of parameters obtained are J/k_B = +9.4(3) K and g_{iso} = 2.29(1) using the data above 20 K, in order to minimize anisotropy effects or intermolecular antiferromagnetic exchange interactions (Figure 3).[8,11,18,22]

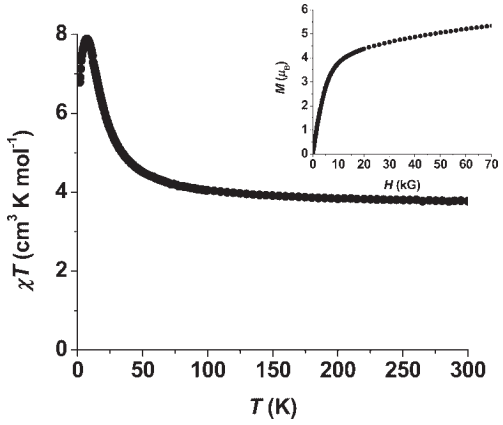

Figure 3. Temperature dependence of the χT product for **2** at H = 0.1 T. Inset: Field dependence of the magnetization at 1.8 K.

When non-zero inter complex exchange interactions (J') are also taken into consideration using a mean field approximation,[24–26] the data can not be adequately reproduced between 300 and 1.8 K (Figure S2; supporting information; for supporting information see also the footnote on the first page of this paper),[18] indicating that additional factors (e.g. anisotropy, second-neighbor Fe···Fe or Ni···Ni magnetic interactions) may also be relevant. The magnitude of the magnetic Ni–Fe exchange coupling constant calculated for **2** is slightly larger than that determined for **1** [7.6 K],[8,18] being comparable to values found for other tri- and tetranuclear complexes containing Ni^{II} and $[(Tp^{R,R})Fe^{III}(CN)_3]^-$ (R = H, Me) and centers.[6–9,24–26] Confirmation of an S = 3 ground state is obtained in the M vs. H_{dc} data at 1.85 K because the magnetization is nearly saturated at 7 T, approaching a maximum value of 6 μ_B (see inset in Figure 3).[18]

The temperature dependence of the ac susceptibility for **2** was measured at several different frequencies at H_{dc} = 0 Oe (Figure 4). The ac susceptibility is frequency-dependent suggesting that the **2** exhibits slow relaxation of the magnetization. From the data shown in Figure 3, the relaxation time τ, can be determined from the maximum of $\chi''(T)$.[4] The relaxation time for **2** follows an Arrhenius law with an energy gap of 20.4 K and $\tau_0 = 5.4 \times 10^{-9}$ s (see inset in Figure S5 in the supporting information). As in many complexes that exhibit slow relaxation of the magnetization, it is likely that the observed energy barrier takes an effective value, resulting from a "short-cut" of the thermal barrier by quantum tunnelling of the magnetization (QTM). In zero field, the $\pm m_S$ states have the same energy and QTM between these pairs of levels is possible. When a magnetic field is applied, the $m_S < 0$ and $m_S > 0$ levels decrease and increase respectively in energy, preventing quantum tunneling between the $\pm m_S$ states.[4]

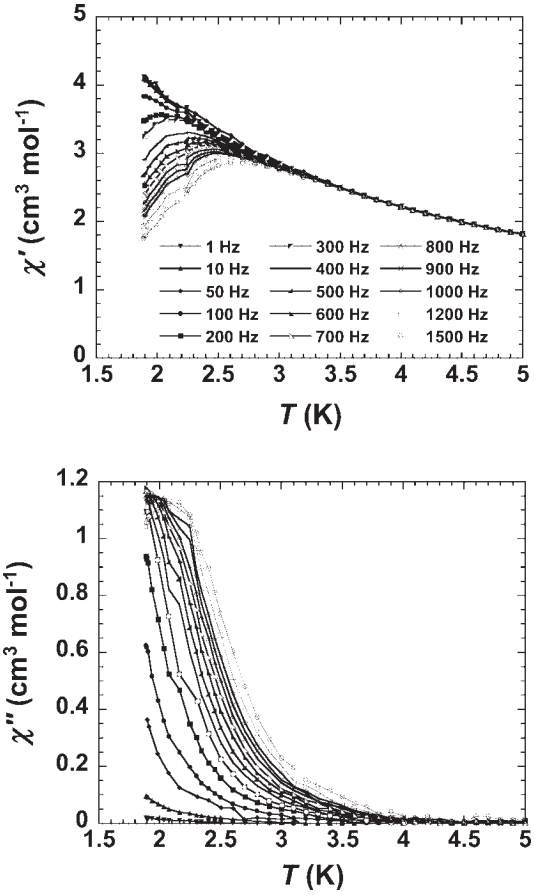

Figure 4. Temperature dependence of the real (χ', top) and imaginary (χ'', bottom) components of the ac susceptibility for **2** (H_{dc} = 0 Oe; H_{ac} = 3 Oe) between 1 and 1500 Hz.

To further investigate the activated behavior of **2**, we performed ac susceptibility measurements under several applied dc magnetic fields (Figures 5, 6, and S3, S4 in the supporting information).[18] At 1.85 K, the characteristic frequency (maximum of the χ'' vs. ν plot) decreases rapidly from 600 Hz at 0 Oe, approaches a nearly constant value of 2 Hz at 4000 Oe, and disappears when H_{dc} ca. 14000 Oe, as expected when the magnetization is almost saturated (Figure 5). As shown by this result, the QTM relaxation pathway remains efficient even at 1.85 K in zero-field. As expected for a SMM that exhibits fast quantum tunneling of the magnetization (for H_{dc} = 0), the application of non-zero magnetic fields increases the magnetization relaxation time (i.e. relaxation mode frequency decreases with increasing H_{dc}). For **2**, the relaxation time can be estimated using the ac measurements under 4000 Oe, which follow Arrhenius behavior with $\tau_0 = 8.4 \times 10^{-8}$ s and an effective energy gap of 25.7 K (Figure 6). This value allows for a rough estimation of the uniaxial anisotropy and affords $D/k_B \approx -2.9$ K.[18]

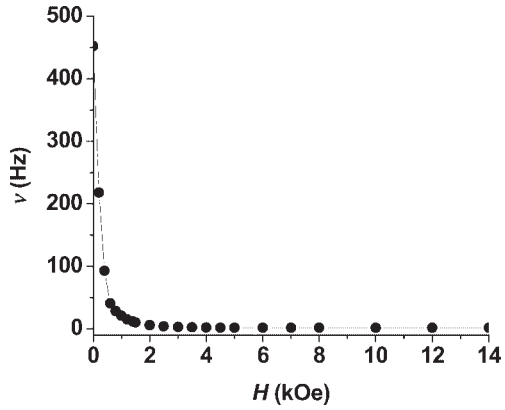

Figure 5. Field dependence of the characteristic frequency at 1.85 K.

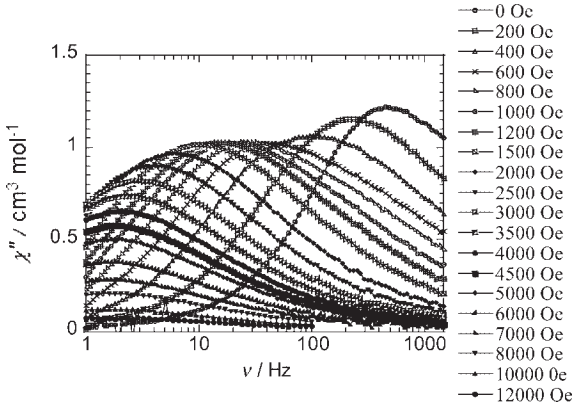

Figure 6. Frequency dependence of χ'' at 1.85 K under various applied H_{dc} for **2**.

To date, few systematic studies of cyanide-bridged polynuclear complexes that exhibit slow relaxation of the magnetization have been described for a given structural archetype. We previously reported that in $\{Fe^{III}_2Ni^{II}\}$ complexes bending of the M–C≡N–M′ bridges significantly impacts the superexchange efficiency (J) and anisotropy energy barrier (Δ): nonlinear cyanide bridges usually afford smaller J and Δ values.[24–26,30] We had anticipated that structural distortion of the $\{Fe^{III}_2Ni^{II}_2(\mu\text{-}CN)_4\}$ core and concomitant coordination spheres of the metal ions present would afford similar changes in exchange coupling (J), zero-field splitting (D), and effective barrier heights (Δ_{eff}) of the tetranuclear complexes.

However, we were surprized to find that despite having bent Fe–C≡N–Ni units, **2** exhibits ferromagnetic superexchange interactions ($J > 0$) that are slightly larger than those in **1**.[7] Recent DFT calculations for $\{Fe^{III}_2M^{II}_2(\mu\text{-}CN)_4\}$ complexes (M^{II} = Mn, Co, Ni) suggest that the total magnetic anisotropy of the ground state is largely dependent on transverse anisotropy contributions (ca. 15–36%) to the total longitudinal anisotropy, originating from the orbital contributions of the S = 1/2 Fe^{II} centers.[31] In comparison to $Mn_{12}O_{12}(O_2CMe)_{16}(OH_2)_4$ faster quantum tunneling rates, larger D parameters, and angular-momentum contributions to the magnetic ground state (ca. 4 times) are found for **1** and **2**. The ac susceptibility measurements (H_{dc} = 0) indicate **1** and **2** exhibit similar behavior suggesting that both exhibit slow relaxation of the magnetization. We postulate that the single-ion anisotropy contributions of the Ni^{II} centers are of minor importance in tuning the magnetic relaxation behavior of the these tetranuclear complexes.

Conclusions

In summary, we have described the preparation, structures, and magnetic properties of two rectangular cyanide-bridged $\{Fe^{III}_2Ni^{II}_2\}$ complexes that exhibit slow relaxation of the magnetization. We propose that steric repulsion between the $[(Tp^*)Fe^{III}(CN)_3]^-$ and $[Ni^{II}(bipy)_2]^{2+}$ units affords bent cyanide bridges that are *cis* to each other affording a distorted-octahedral Ni^{II} coordination environment in **2**. Surprisingly, despite severe structural distortion of the $\{Fe^{III}_2Ni^{II}_2(CN)_4\}$ core, **2** exhibits slow frequency-dependent magnetization relaxation behavior that is comparable to **1**, a more symmetrical analog. We tentatively propose that for **1** and **2** the height of the magnetization reversal barrier is largely dependent on the single-ion anisotropy contributions of the low-spin Fe^{III} centers, while the Ni^{II} centers appear to be of minor importance. A future report will describe how spin-orbit coupling and orbital contributions of the magnetic ions contribute to the overall magnetic anisotropy and relaxation behavior of several polynuclear cyanide-bridged complexes.[31]

Experimental Section

General: All operations were conducted while dark in a vacuum or under argon using standard Schlenk and drybox techniques. Transfers of solutions containing cyanides were carried out through stainless steel cannulas. The salts $[NEt_4][(Tp^*)Fe^{III}(CN)_3]$,[7] $Ni(OTs)_2$,[32] and **1**[21] were prepared according to modified literature methods. Diethyl ether was distilled from sodium/benzophenone and sparged with argon prior to use. DMF (Baker) was dried with activated Linde 13-X molecular sieves and sparged with argon prior to use. 2,2′-Bipyridine (Aldrich) was used as received.

Physical Methods: The IR spectra were recorded as Nujol mulls between KBr plates with a Mattson Galaxy 5200 FTIR instrument. The dc magnetic measurements were obtained using crushed, single crystals of **2**, on a Quantum Design MPMS-XL SQUID magnetometer, operating between 1.8 and 300 K, in a 0.1 T static magnetic field. Initial ac measurements were obtained over 1.8 to 5 K (H_{dc} = 0 Oe and H_{ac} = 3 Oe) and between 1 and 1500 Hz; additional measurements were obtained at temperatures between 1.8 and 5 K (H_{dc} = 0, 1000 and 4000 Oe; H_{ac} = 3 Oe). Magnetic data were corrected for the sample holder diamagnetism, while diamagnetic contributions from the samples were estimated using Pascal's constants.[36] Microanalyses were performed by Robertson Microlit Laboratory.

X-ray Structural Studies: Crystals of **2** were grown from DMF/Et_2O solutions of **1**[7] treated with 4 equiv. of 2,2′-bipyridine. X-ray diffraction data were collected at 90.0(2) K with a Bruker X8 Proteum rotating-anode CCD diffractometer with graphite-monochromated Cu-K_α (λ = 1.54178 Å) radiation from irregular shaped crystals, mounted in Paratone-N oil on glass fibers. Initial cell parameters

were obtained (DENZO)[33] from ten 1° frames and were refined via a least-squares scheme using all data-collection frames (SCALEPACK).[33] Lorentz/polarization corrections were applied during data reduction. The structures were solved by direct methods (SHELXS97) and completed by difference Fourier methods (SHELXL97).[34] Refinement was performed against F^2 by weighted full-matrix least-squares (SHELXL97)[34] and empirical absorption corrections (either SCALEPACK[33] or SADABS[34]) were applied. Hydrogen atoms were found in difference maps and subsequently placed at calculated positions using suitable riding models with isotropic displacement parameters derived from their carrier atoms. Non-hydrogen atoms were refined with anisotropic displacement parameters. Atomic scattering factors were taken from the International Tables for Crystallography vol. C.3.[35] Crystal data, relevant details of the structure determinations, and selected geometrical parameters are provided in the supporting information.[18]

Synthesis of 2: Treatment of $\{[(Tp^*)Fe^{III}(CN)_3]_2[Ni^{II}(DMF)_4]_2[OTf]_2\}\cdot 2DMF$ (**1**) (0.949 g, 0.50 mmol) in MeOH/CH_3CN [30 mL, 1:1 (v/v)] with 2,2′-bipyridine (0.312 g, 2.00 mmol) afforded a red solution that was layered with Et_2O (20 mL) and allowed to stand for 3 d. The red needles were collected by filtration, washed with CH_3CN (5 mL) and Et_2O (3 × 5 mL), and dried in air overnight. Yield: 0.546 g (55.3%). $C_{78}H_{84}B_2F_6Fe_2N_{26}Ni_2O_{10}S_2$ (1974.53): calcd. C 47.40, H 4.30, N 18.43; found C 47.43, H 4.10, N 18.76. IR (Nujol): $\tilde{\nu}$ = 3460 (br., m), 2952 (vs), 2926 (vs), 2854 (vs), 2553 (m), 2158 (vs), 2128 (m), 1634 (m), 1598 (s), 1575 (m), 1567 (m), 1543 (vs), 1489 (s), 1447 (vs), 1417 (vs), 1375 (vs), 1310 (m), 1285 (vs), 1256 (vs), 1227 (vs), 1203 (vs), 1162 (vs), 1108 (m), 1062 (vs), 1031 (vs), 988 (m), 867 (m), 815 (m), 806 (m), 775 (vs), 738 (s), 722 (m), 692 (m), 641 (vs), 575 (m), 544 (w), 517 (m), 440 (m), 429 (m), 410 (m) cm^{-1}.

Supporting Information (see also the footnote on the first page of this article): Crystallographic data (CIF format) and additional magnetic data for **2**.

CCDC-634744 contains the supplementary crystallographic data for this paper. These data can be obtained free of charge from The Cambridge Crystallographic Data Centre via www.ccdc.cam.ac.uk/data_request/cif.

Acknowledgments

S. M. H. gratefully acknowledges the Kentucky Science and Engineering Foundation (Grants KSEF-621-RDE-006 and KSEF-992-RDE-008) and the National Science Foundation (CAREER CHE-0645414) for financial support. R. C. thanks MAGMANet (NMP3-CT-2005-515767), the French Centre National de Recherches Scientifique (CNRS), the University of Bordeaux 1, and the Conseil Régional d'Aquitaine for financial support. G. T. Y. thanks the National Science Foundation (CHE-0210395) for partial financial support. S. M. H. and R. C. are also grateful to Eugenio Coronado and Jeffery R. Long for providing the MAGPACK and ANISOFIT programs, respectively.

[1] M. N. Leuenberger, D. Loss, *Nature* **2001**, *410*, 789–793.
[2] W. Wernsdorfer, N. Aliaga-Alcalde, D. N. Hendrickson, G. Christou, *Nature* **2002**, *416*, 406–409.
[3] S. Hill, R. S. Edwards, N. Aliaga-Alcalde, G. Christou, *Science* **2003**, *302*, 1015–1018.
[4] R. Sessoli, D. Gatteschi, *Angew. Chem. Int. Ed.* **2003**, *42*, 268–297, and references therein.
[5] L. M. C. Beltran, J. R. Long, *Acc. Chem. Res.* **2005**, *38*, 325–334, and references therein.
[6] D. Li, S. Parkin, G. Wang, G. T. Yee, R. Clérac, W. Wernsdorfer, S. M. Holmes, *J. Am. Chem. Soc.* **2006**, *128*, 4214–4215.
[7] D. Li, S. Parkin, G. Wang, G. T. Yee, A. V. Prosvirin, S. M. Holmes, *Inorg. Chem.* **2005**, *44*, 4903–4905.
[8] D. Li, R. Clérac, S. Parkin, G. T. Yee, S. M. Holmes, *Inorg. Chem.* **2006**, *46*, 5251–5253.
[9] D. Li, R. Clérac, S. Parkin, G. Wang, G. T. Yee, S. M. Holmes, *Inorg. Chem.* **2006**, *46*, 7569–7571.
[10] E. J. Schelter, A. V. Prosvirin, K. R. Dunbar, *J. Am. Chem. Soc.* **2004**, *126*, 15004–15005.
[11] S. Wang, J.-L. Zou, H.-C. Zhou, H. J. Choi, Y. Ke, J. R. Long, X.-Z. You, *Angew. Chem. Int. Ed.* **2004**, *43*, 5940–5943.
[12] C. P. Berlinguette, D. Vaughn, C. Cañada-Vilalta, J. R. Galán-Mascarós, K. R. Dunbar, *Angew. Chem. Int. Ed.* **2003**, *42*, 1523–1526.
[13] A. V. Palii, S. M. Ostrovsky, S. I. Klokishner, B. S. Tsukerblat, K. R. Dunbar, J. R. Galán-Mascarós, *J. Am. Chem. Soc.* **2004**, *126*, 16860–16867.
[14] E. J. Schelter, A. V. Prosvirin, W. M. Reiff, K. R. Dunbar, *Angew. Chem. Int. Ed.* **2004**, *43*, 4912–4915.
[15] J. J. Sokol, A. G. Hee, J. R. Long, *J. Am. Chem. Soc.* **2002**, *124*, 7656–7657.
[16] G. Rogez, J.-N. Rebilly, A.-L. Barra, L. Sorace, G. Blondin, N. Kirchner, M. Duran, J. van Slageren, S. Parsons, L. Ricard, A. Marvilliers, T. Mallah, *Angew. Chem. Int. Ed.* **2005**, *44*, 1876–1879.
[17] a) S. Accorsi, A.-L. Barra, A. Caneschi, G. Chastanet, A. Cornia, A. C. Fabretti, D. Gatteschi, C. Mortalò, E. Olivieri, F. Parenti, P. Rosa, R. Sessoli, L. Sorace, W. Wernsdorfer, L. Zobbi, *J. Am. Chem. Soc.* **2006**, *128*, 4742–4755; b) C. J. Milios, A. Vinslava, P. A. Wood, S. Parsons, W. Wernsdorfer, G. Christou, S. P. Perepes, E. K. Brechin, *J. Am. Chem. Soc.* **2007**, *129*, 8–9.
[18] See the Supporting Information.
[19] J. Y. Yang, M. P. Shores, J. J. Sokol, J. R. Long, *Inorg. Chem.* **2003**, *42*, 1403–1419.
[20] J. Kim, S. Han, I.-K. Cho, K. Y. Choi, M. Heu, S. Yoon, B. J. Suh, *Polyhedron* **2004**, *23*, 1333–1339.
[21] D. Li, S. Parkin, G. Wang, G. T. Yee, S. M. Holmes, *Inorg. Chem.* **2006**, *45*, 1951–1959.
[22] D. Li, S. Parkin, G. Wang, G. T. Yee, S. M. Holmes, *Inorg. Chem.* **2006**, *45*, 2773–2775.
[23] Crystal and structure refinement parameters: **2**, $C_{78}H_{84}B_2F_6Fe_2N_{26}Ni_2O_{10}S_2$, $P\bar{1}$, Z = 8, a = 11.3573(3) Å, b = 13.5093(3) Å, c = 14.7470(4), α = 96.713(1)°, β = 98.668(1)°, γ = 99.237(1)°, V = 2184.6(1) $Å^3$, R_1 = 0.0662, wR_2 = 0.1823.
[24] Y. Nakamura, M. Yonemura, K. Arimura, N. Usuki, M. Ohba, H. Okawa, *Inorg. Chem.* **2001**, *40*, 3739–3744.
[25] S. Wang, J.-L. Zuo, H.-C. Zhou, Y. Song, X.-Z. You, *Inorg. Chim. Acta* **2005**, *358*, 2101–2106.
[26] S. Wang, J.-L. Zuo, H.-C. Zhou, Y. Song, S. Gao, X.-Z. You, *Eur. J. Inorg. Chem.* **2004**, 3681–3687.
[27] J. H. van Vleck, *The Theory of Electric and Magnetic Susceptibility*, Oxford University Press, New York, **1932**.
[28] K. Kambe, *J. Phys. Soc. Jpn.* **1950**, *5*, 48–51.
[29] K. Nakamoto, *Infrared and Raman Spectra of Inorganic and Coordination Compounds*, 5th ed., Part B, Wiley, New York, **1997**.
[30] M. P. Shores, J. J. Sokol, J. R. Long, *J. Am. Chem. Soc.* **2002**, *124*, 2279–2292.
[31] K. Park, S. M. Holmes, *Phys. Rev. B* **2006**, *74*, 224440-1–224440-10.
[32] S. M. Holmes, S. G. McKinley, G. S. Girolami, *Inorg. Synth.* **2002**, *33*, 91–103.
[33] Z. Otwinowski, W. Minor, *Methods Enzymol.* **1997**, *276*, 307–326.

[34] G. M. Sheldrick, *SADABS, An empirical absorption correction program*, Bruker Analytical X-ray Systems, Madison, Wisconsin, **1996**; G. M. Sheldrick, *SHELX-97, Programs for Crystal Structure Solution and Refinement*, University of Göttingen, Germany, **1997**.
[35] International Tables for Crystallography, vol. C, Kluwer Academic Publishers, Dordrecht, The Netherlands, **1992**.
[36] O. Kahn, *Molecular Magnetism*, VCH Publishers, New York, **1993**.

Received: September 5, 2006
Published Online: February 22, 2007

